Contribution from the Department of Chemistry,
Michigan State University, East Lansing, Michigan 48824

Partitioning of the Electrochemical Excitation Energy in the Electrogenerated Chemiluminescence of Hexanuclear Molybdenum and Tungsten Clusters

Robert D. Mussell and Daniel G. Nocera*,†

Received November 14, 1989

The electrogenerated chemiluminescence (ecl) of the hexanuclear cluster complexes $M_6X_8Y_6^{2-}$ (M = Mo, W; X, Y = Cl, Br, I) in dichloromethane has been investigated. Overall ecl quantum yields and relative production yields of electronically excited $Mo_6Cl_{14}^{2-}$ and $W_6X_8Y_6^{2-}$ (X, Y = Cl, Br, I; X = Cl, Y = Br; X = I, Y = Br) have been measured for the annihilation of $Mo_6Cl_{14}^{3-}$ and $W_6X_8Y_6^{-}$. In all cases, equal or nearly equal partitioning of the electrochemical excitation energy is observed. This result suggests that the rates of electron transfer of the trianion $Mo_6Cl_{14}^{3-}$ and monoanion $W_6X_8Y_6^{-}$ to produce their respective excited states are equal owing to similar electronic coupling and activation barriers for $Mo_6Cl_{14}^{2-*} \leftrightarrow Mo_6Cl_{14}^{3-}$ and $W_6X_8Y_6^{2-*} \leftrightarrow W_6X_8Y_6^{-}$ exchange. Consistent with partitioning studies are the electron-transfer reactions of $Mo_6Cl_{14}^{2-*}$ with aromatic amine donors (D) and $W_6X_8Y_6^{2-*}$ with aromatic nitro or quinone acceptors (A), to produce $Mo_6Cl_{14}^{3-}$ and $W_6X_8Y_6^{-}$, respectively. Slopes of −0.49 and −0.51 for the plots of $RT \ln k_q$ vs the free energy driving force for $Mo_6Cl_{14}^{2-*}/D$ and $W_6X_8Y_6^{2-*}/A$ electron transfers, respectively, are in the accordance with the predictions of Marcus' theory. As originally inferred from equal partitioning ratios, analysis of the quenching rates reveals that $Mo_6Cl_{14}^{2-*} \leftrightarrow Mo_6Cl_{14}^{3-}$ and $W_6X_8Y_6^{2-*} \leftrightarrow W_6X_8Y_6^{-}$ exchange reactions possess similar electron-transfer activation barriers ($\lambda(W_6X_8Y_6^{2-*}/W_6X_8Y_6^{-}) = 1.01$ eV and $\lambda(Mo_6Cl_{14}^{2-*}/Mo_6Cl_{14}^{3-}) = 1.11$ eV). These ecl partitioning and quenching results establish that the $M_6X_8Y_6^{-}$ and $M_6X_8Y_6^{3-}$ electrogenerated intermediates contribute equally to the excited-state production in the ecl reactions of these cluster ions.

Introduction

The generation of electronically excited products by electron transfer between electrochemically (electrogenerated chemiluminescence, ecl) or chemically (chemiluminescence, cl) generated intermediates is a useful probe of biological and chemical oxidation–reduction processes.[1,2] Not only do reactions along electroluminescent and chemiluminescent pathways allow for the detection of reactive intermediates[1-11] and provide insight into the mode of their formation,[1-3,12-18] but they also play an important role in the elucidation of the factors that govern highly exergonic electron-transfer reactions.[19-21] In regard to this latter issue, classical[22] and quantum-mechanical theories[23,24] predict that electron annihilation of oxidized and reduced reactants to generate the excited state will proceed in the Marcus normal regime (i.e. increasing rate with an increasingly negative free energy driving force ΔG) whereas direct reaction to ground state occurs in the inverted regime (i.e. decreasing rate with more negative ΔG). Recent studies by us[25] and others[26] have exploited ecl and cl yields, respectively, for the formation of excited- and ground-state products to shed light on mechanistic aspects governing electron exchange in the inverted and normal regimes. Inasmuch as electron-transfer parameters such as distance, driving force, and reorganizational energy are manifest to determining the yield between excited-state and ground-state products, these factors will also bear directly on the partitioning of the electrochemical or chemical excitation energy among the excited-state products of ecl or cl pathways, respectively. In a simple ecl or cl annihilation reaction, oxidized or reduced reactant can be brought to the excited state ($M^+ + M^- \rightarrow M^* + M$; $M^+ + M^- \rightarrow M + M^*$). Energy partitioning between these two parentages is ultimately related to differences in activation barrier heights arising from dissimilar reorganizational energies and disparate electronic factors for the two distinct electron-transfer pathways. Hence production of M^* from oxidized or reduced reactant is of fundamental significance because it provides insight into the electron-transfer properties of highly energetic intermediates M^+ and M^-. Nevertheless the issue of partitioning of electrochemical or chemical excitation energy in ecl or cl annihilation reactions has heretofore eluded identification because there has been no simple way of labeling the oxidized or reduced reactant.

One approach to determining partitioning ratios among excited-state products is to generate oxidized or reduced reactants from parent molecules that possess distinct luminescent excited states, thereby allowing the parentage of the excited state to be identified with facility. Such an approach has previously been considered for the ecl reactions of RuL_3^{2+}/RuL'_3^{2+} (L ≠ L'; L,

† Alfred P. Sloan Fellow and NSF Presidential Young Investigator.

(1) (a) Tachikawa, H.; Faulkner, L. R. In *Laboratory Techniques in Electroanalytical Chemistry*; Kissinger, P. T., Heineman, W. R., Eds.; Marcel Dekker: New York, 1984; Chapter 23. (b) Faulkner, L. R.; Glass, R. S. *Chemical and Biological Generation of Excited States*; Adam, W., Gilento, G., Eds.; Academic: New York, 1982. (c) Faulkner, L. R. *Methods Enzymol.* **1978**, *57*, 494-526.
(2) Weller, A.; Zachariasse, K. *Chemiluminescence and Bioluminescence*; Cormier, M., Hercules, D. M., Lee, J., Eds.; Plenum: New York, 1973.
(3) Park, S.-M.; Tryk, D. A. *Rev. Chem. Intermed.* **1981**, *4*, 43-79.
(4) Vogler, A.; Kunkely, H. *ACS Symp. Series* **1987**, *333*, 155-168.
(5) Balzani, V.; Bolletta, F. *Comments Inorg. Chem.* **1983**, *2*, 211-226.
(6) (a) Lee, C. W.; Ouyang, J.; Bard, A. J. *J. Electroanal. Chem. Interfacial Electrochem.* **1988**, *244*, 319-324. (b) Ouyang, J.; Bard, A. J. *Bull. Chem. Soc. Jpn.* **1988**, *61*, 17-24. (c) Wheeler, B. L.; Nagasubramanian, G.; Bard, A. J.; Schechtman, L. A.; Dininny, D. R.; Kenney, M. E. *J. Am. Chem. Soc.* **1984**, *106*, 7404-7410. (d) Gonzales-Velasco, J.; Rubinstein, I.; Crutchley, R. J.; Lever, A. B. P.; Bard, A. J. *Inorg. Chem.* **1983**, *22*, 822-825.
(7) Vogler, A.; Kunkely, H. *Angew. Chem., Int. Ed. Engl.* **1984**, *23*, 316-317.
(8) (a) Ouyang, J.; Zietlow, T. C.; Hopkins, M. D.; Fan, F.-R. F.; Gray, H. B.; Bard, A. J. *J. Phys. Chem.* **1986**, *90*, 3841-3844. (b) Kim, J.; Fan, F.-R. F.; Bard, A. J.; Che, C.-M.; Gray, H. B. *Chem. Phys. Lett.* **1985**, *121*, 543-546.
(9) Bonafede, S.; Ciano, M.; Bolletta, F.; Balzani, V.; Chassot, L.; Zelewsky, A. *J. Phys. Chem.* **1986**, *90*, 3836-3841.
(10) (a) Ludvik, J.; Volke, J. *Anal. Chim. Acta* **1988**, *209*, 69-78. (b) Ludvik, J.; Volke, J.; Pragst, F. *J. Electroanal. Chem. Interfacial Electrochem.* **1986**, *215*, 179-190. (c) Ludvik, J.; Pragst, F.; Volke, J. *J. Electroanal. Chem. Interfacial Electrochem.* **1984**, *180*, 141-156.
(11) (a) Kane-Maguire, N. A. P.; Wright, L. L.; Guckert, J. A.; Tweet, W. S. *Inorg. Chem.* **1988**, *27*, 2905-2907. (b) Kane-Maguire, N. A. P.; Guckert, J. A.; O'Neill, P. J. *Inorg. Chem.* **1987**, *26*, 2340-2242.
(12) (a) Kim, J.; Faulkner, L. R. *J. Am. Chem. Soc.* **1988**, *110*, 112-119. (b) Kim, J.; Faulkner, L. R. *J. Electroanal. Chem. Interfacial Electrochem.* **1988**, *242*, 107-121. (c) Kim, J.; Faulkner, L. R. *J. Electroanal. Chem. Interfacial Electrochem.* **1988**, *242*, 123-129.
(13) (a) Pragst, F.; Niazymbetov, M. *J. Electroanal. Chem. Interfacial Electrochem.* **1986**, *197*, 245-264. (b) Pragst, F. *Z. Chem.* **1978**, *18*, 41-50.
(14) Gonzalez-Velasco, J. *J. Phys. Chem.* **1988**, *92*, 2202-2207.
(15) Glass, R. S.; Faulkner, L. R. *J. Phys. Chem.* **1981**, *85*, 1160-1165.
(16) Luttmer, J. D.; Bard, A. J. *J. Phys. Chem.* **1981**, *85*, 1155-1159.
(17) Itoh, K.; Honda, K.; Sukigara, M. *Electrochim. Acta* **1979**, *24*, 1195-1198.
(18) Rossella, B.; Bard, A. J. *J. Electroanal. Chem. Interfacial Electrochem.* **1987**, *238*, 277-295.
(19) Faulkner, L. R. *Int. Rev. Sci.: Phys. Chem., Ser. Two* **1975**, *9*, 213-263.
(20) Bock, C. R.; Connor, J. A.; Gutierrez, A. R.; Meyer, T. J.; Whitten, D. G.; Sullivan, B. P.; Nagle, J. K. *J. Am. Chem. Soc.* **1979**, *101*, 4815-4824.
(21) Marcus, R. A.; Siders, P. *J. Phys. Chem.* **1982**, *86*, 622-630.
(22) Marcus, R. A. *J. Chem. Phys.* **1965**, *43*, 2654-2657.

0020-1669/90/1329-3711$02.50/0

L′ = polypyridyl) systems,[27] but electrochemical partitioning studies have been hampered for the most part by (i) the inability to selectively generate the oxidized and reduced reactants from distinct parent molecules owing to the similarity of the $RuL_3^{+/2+}$ and $RuL'_3{}^{+/2+}$ couples and/or (ii) insufficient electrochemical excitation energy to produce either of the excited-state products. In this regard, we soon realized during our investigations of the ecl reactivity of $Mo_6Cl_{14}^{2-}$ that the more general class of $M_6X_8Y_6^{2-}$ (M = Mo, W; X = Cl, Br, I) complexes is particularly well-suited for partitioning studies. The $M_6X_8Y_6^{2-*}$ excited state can be generated from either $M_6X_8Y_6^-$ or $M_6X_8Y_6^{3-}$, and the problems inherent in the design of reliable multicomponent ecl systems are circumvented. Namely, the ability to control the $M_6X_8Y_6^{-/2-}$ and $M_6X_8Y_6^{2-/3-}$ redox couples and $M_6X_8Y_6^{2-*}$ excited-state properties with judicious choice of M, X, and Y[28] permits the desired oxidized or reduced precursors to cleanly be established and their reaction to excited state to be detected. Moreover the relatively large driving force associated with typical $M_6X_8Y_6^{-/3-}$ electron transfers[29] ensures that either excited state can be, in principle, produced upon annihilation. We now report studies on the partitioning of the electrochemical excitation energy in the ecl chemistry of $M_6X_8Y_6^{2-}$ ions. Analysis of the partitioning ratios for the distribution of the electrochemical excitation energy between different $M_6X_8Y_6^{2-}$ products yields direct information on the electron-transfer properties of the reactive $M_6X_8Y_6^-$ and $M_6X_8Y_6^{3-}$ redox intermediates.

Experimental Section

Materials. The tetrabutylammonium salt of $Mo_6Cl_{14}^{2-}$, aromatic acceptors and donors used in quenching studies, supporting electrolyte, and solvents were prepared and purified as previously described.[25a] The tetrabutylammonium salts of other $W_6X_8Y_6^{2-}$ ions were obtained directly from the appropriate tungsten dihalides.

The method of Dorman and McCarley[30] was used with slight modification to prepare tungsten dichloride. In a typical reaction of 15 g of WCl_6, 1.35 g of Al metal, 6.75 g of NaCl, and 10.00 g of $AlCl_3$ were added in a drybox to a quartz reaction tube. The tube was capped with a rubber septum, removed from the drybox, connected to a high-vacuum manifold, evacuated for 1 h, and then flame-sealed under dynamic vacuum. The contents were thoroughly mixed, and the reaction vessel was placed into a high-temperature furnace, which was heated to a temperature of 210 °C. After 6 h, the temperature was raised to 450 °C over a 3-h period, held at 450 °C for 9 h, and finally raised to 550 °C, where it was held for 24 h. The tube was allowed to cool to room temperature and its contents were collected. (*Caution*! Violent explosions sometimes resulted upon opening the tube.) The black fused solid was dissolved in a 6 M HCl/ethanol solution, and the mixture was filtered to remove any insoluble reaction products. The light yellow filtrate was reduced in volume, and upon cooling, greenish yellow crystals of $(H_3O)_2W_6Cl_{14}$ formed. The crystals were collected and heated in a furnace at 350 °C for 2 h under a dynamic vacuum to yield W_6Cl_{12}. The tetrabutylammonium salt of $W_6Cl_{14}^{2-}$ was prepared by addition of NBu_4Cl to an ethanol/HCl solution of W_6Cl_{12}. The precipitate was collected, washed with water and ethanol, and recrystallized several times from CH_2Cl_2.

Tungsten dibromide was prepared in a manner similar to that for tungsten dichloride. To the quartz reaction tube were added in the drybox 15 g of WBr_5, 0.72 g of Al metal, 7.50 g of NaBr, and 13.0 g of $AlBr_3$. The reaction conditions were identical with those used for the preparation of W_6Cl_{12}. The black solid product was dissolved in a solution of 6 M HBr and ethanol; the solution was filtered and evaporated over gentle heating to near dryness. The residue was collected and dissolved in ethanol, and the insoluble alkali-metal salts were removed by filtration. The ethanol was allowed to evaporate to afford greenish crystals of $W_6Br_{12}(HOCH_2CH_3)_2$. The tetrabutylammonium salt of $W_6Br_{14}^{2-}$ was prepared by addition of NBu_4Br to an ethanol/HBr solution of $W_6Br_{12}(HOCH_2CH_3)_2$. $(NBu_4)_2W_6Br_{14}$ was recrystallized several times from acetonitrile solutions.

Tungsten diiodide was prepared by the halide exchange of WCl_2.[31] A quartz reaction tube was charged with 1.00 g of $K_2W_6Cl_{14}$, 9.97 g of KI, and 3.60 g of LiI in the drybox. The reaction tube was removed from the drybox, sealed under dynamic vacuum (10^{-6} Torr), and placed into a furnace. The temperature of the furnace was raised over a 1.5-h period to 550 °C, and the reaction was allowed to proceed for 1 h. Upon cooling to room temperature, the tube was opened carefully. (*Caution*! Violent explosions sometimes resulted.) The black solid was washed with water to remove alkali-metal salts and iodine. The remaining yellow-brown solid was extracted with ethanol to give a deep golden brown solution of W_6I_{12}, which was isolated by evaporation of ethanol and subsequent heating of the solid under vacuum. The tetrabutylammonium salt of $W_6I_{14}^{2-}$ was obtained by addition of NBu_4I to an ethanol solution of W_6I_{12}. The dark yellow powder was collected, washed several times with ethanol, and recrystallized several times from dry CH_3CN to yield pure $(NBu_4)_2W_6I_{14}$.

Mixed tungsten halide clusters, $W_6X_8Y_6^{2-}$ (X = Cl, Y = Br; X = I, Y = Br), were prepared by dissolving $(W_6X_8)X_4$ in ethanol and 6 M hydrohalic acid HY.[30] The solubility of the cluster in HY decreases along the series HCl > HBr > HI, and thus a larger amount of ethanol must be added for the latter hydrohalic acids. To ensure complete exchange of axial halides, the resultant solution was evaporated to near dryness with moderate heating. When $W_6X_8Y_6^{2-}$ was prepared, gentle heating under a vacuum aspirator was required. An insoluble precipitate formed when the solution was heated too rigorously. The residue, collected from solvent evaporation, was redissolved in ethanol/6 M HY solutions. The tetrabutylammonium salt was obtained by addition of excess NBu_4Y to the ethanol/HY solution. The mixed-halide tungsten clusters $(NBu_4)_2W_6X_8Y_6$ were recrystallized several times from either dry CH_3CN or CH_2Cl_2.

A thorough characterization of all the molybdenum and tungsten cluster systems was performed by negative-ion fast atom bombardment mass spectrometry (FABMS). The technique utilizes a 10-keV xenon beam which bombards a sample placed in a high viscosity, low vapor pressure matrix. The energy from the beam is transferred to the matrix, which causes desorption of matrix sample ions into the gas phase. The negative ions generated during the absorption process were isolated and recorded to give fingerprint spectra of each cluster. FABMS is a superior analytical method for the synthesized clusters because substituted halide clusters are easily detected. The detailed experimental results and a general discussion of the usefulness of this technique will be presented elsewhere.[32]

Quenching Measurements. Electron-transfer-quenching rate constants for the reaction of $Mo_6Cl_{14}^{2-*}$ with aromatic amines and $W_6X_8Y_6^{2-*}$ ions with nitroaromatic and quinone compounds were determined from Stern–Volmer analysis of the cluster ion luminescence intensity and lifetime.[33] Intensity (λ_{exc} = 436 nm) and lifetime (λ_{exc} = 355 nm from a Nd:YAG with fwhm = 8 ns) measurements were determined on equipment designed and constructed at Michigan State University.[25a,34] The quenching rates calculated from intensity and lifetime methods for a given system were within 5% of each other. The Stern–Volmer lifetime method was used to study the energy-transfer quenching of $Mo_6Cl_{14}^{2-*}$ and $W_6X_8Y_6^{2-*}$ by $W_6X_8Y_6^{2-}$ and $Mo_6Cl_{14}^{2-}$, respectively.

Stern–Volmer experiments were performed on acetonitrile and dichloromethane solutions (μ = 0.1 M (NBu_4PF_6)) containing 3 mM cluster (lumophore) and over a quencher concentration range of 5×10^{-4} to 1×10^{-1} M. Stern–Volmer constants were calculated by using $\tau_0(Mo_6Cl_{14}^{2-*})$ = 160, 180 μs, $\tau_0(W_6Cl_{14}^{2-*})$ = 2.2, 1.5 μs, $\tau_0(W_6Br_{14}^{2-*})$ = 16, 15 μs, $\tau_0(W_6I_{14}^{2-*})$ = 26, 30 μs, $\tau_0(W_6Cl_8Br_6^{2-*})$ = 4.4, 2.3 μs, and $\tau_0(W_6I_8Br_6^{2-*})$ = 27, 22 μs in CH_2Cl_2, CH_3CN at 23 °C. Quenching experiments were performed in a specially constructed high-vacuum cell, consisting of a 1-cm curvette attached to a sidearm terminating with a 10-mL round-bottom flask. Solvents were vacuum distilled into the quenching cell and freeze-pump-thawed three times. All quencher additions were performed under high-vacuum conditions.

Electrochemical and Electrogenerated Chemiluminescence Measurements. Formal reduction potentials of acceptors and donors were determined by cyclic voltammetry by using instrumentation and methods previously described.[25a] Ecl spectra and quantum yield experiments were

(23) Meyer, T. J. *Prog. Inorg. Chem.* **1983**, *30*, 389–440.
(24) Siders, P.; Marcus, R. A. *J. Am. Chem. Soc.* **1981**, *103*, 748–752.
(25) (a) Mussell, R. D.; Nocera, D. G. *J. Am. Chem. Soc.* **1988**, *110*, 2764–2772. (b) Mussell, R. D.; Nocera, D. G. *Polyhedron* **1986**, *5*, 47–50.
(26) Liu, D. K.; Brunschwig, B. S.; Creutz, C.; Sutin, N. *J. Am. Chem. Soc.* **1986**, *108*, 1749–1755.
(27) Bolletta, F.; Bonafede, S. *Pure Appl. Chem.* **1986**, *58*, 1229–1232.
(28) Zietlow, T. C.; Nocera, D. G.; Gray, H. B. *Inorg. Chem.* **1986**, *25*, 1351–1353.
(29) Nocera, D. G.; Gray, H. B. *J. Am. Chem. Soc.* **1984**, *106*, 824–825.
(30) Dorman, W. C.; McCarley, R. E. *Inorg. Chem.* **1974**, *13*, 491–493.
(31) Hogue, R. D.; McCarley, R. E. *Inorg. Chem.* **1970**, *9*, 1354–1359.
(32) Kassel, D. B.; Mussell, R. D.; Allison, J.; Nocera, D. G. To be published.
(33) Balzani, V.; Moggi, L.; Manfrin, M. F.; Bolletta, F. *Coord. Chem. Rev.* **1975**, *15*, 321–433.
(34) Newsham, M. D.; Giannelis, E. P.; Pinnavaia, T. J.; Nocera, D. G. *J. Am. Chem. Soc.* **1988**, *110*, 3885–3891.

Table I. Electrochemical Properties of $Mo_6Cl_{14}^{2-}$ and $W_6X_8Y_6^{2-}$ Cluster Ions Used in Ecl Partitioning Studies[a]

$M_6X_8Y_6^{2-}$ ion	$E_{1/2}(M_6X_8Y_6^{x-/y-})$ vs SCE/V (−,2−)	(2−,3−)[b]
$Mo_6Cl_{14}^{2-}$	+1.36	−1.70
$W_6Cl_8Br_6^{2-}$	+0.99	
$W_6Cl_{14}^{2-}$	+0.93	
$W_6Br_{14}^{2-}$	+0.80	
$W_6I_{14}^{2-}$	+0.57	
$W_6I_8Br_6^{2-}$	+0.56	

[a] All measurements were made in dichloromethane containing 0.1 M tetrabutylammonium hexafluorophosphate at 23 ± 1 °C. [b] The $W_6X_8Y_6^{2-/3-}$ reduction couple is more negative than potentials at which CH_2Cl_2 is reduced.

performed in solutions containing 0.1 M supporting electrolyte (NBu_4PF_6) and equimolar concentrations of $Mo_6Cl_{14}^{2-}$ and $W_6X_8Y_6^{2-}$ ions. Our techniques for the preparation and manipulation of solutions for ecl experiments and the methods for the determination of ecl quantum efficiencies have been described.[22a] Ecl spectra of $Mo_6Cl_{14}^{2-}$/acceptor and -donor systems were recorded between 350 and 1100 nm and between 550 and 1050 nm for $Mo_6Cl_{14}^{2-}/W_6X_8Y_6^{2-}$. Spectra were obtained by interfacing the specially designed electrochemical cell directly to the detection side of the emission spectrometer. The lock-in amplifier was referenced to the ecl signal with the cycle synchronous output of the PAR 175 programmer. The electrochemical cell employed for ecl spectral measurements was a cylindrical, single-compartment high-vacuum cell. A sidearm permitted solvents to be transferred into the cell by vacuum distillation, and two sample chargers allowed cluster and electroactive acceptor or donor to be added independently to the working electrode compartment while maintaining the isolated environment of the electrochemical cell. Two tungsten wires sealed in uranium glass served as electrical leads to the Pt-mesh auxiliary electrode and an Ag-wire quasi-reference electrode. The auxiliary and reference electrodes were positioned parallel to a Pt-disk working electrode (A = 0.707 cm^2) that was positioned perpendicularly to the cylindrical axis of the working compartment. The Pt disk was spectroscopically viewed through a fused-silica window situated on the cylindrical side of the working compartment. After each experiment the Pt-disk electrode was polished with 1-μm diamond paste and 0.05-μm alumina purchased from Bioanalytical Systems. The Pt-disk electrode was positioned at the focal point of the collection lens on the detection side of the emission spectrometer. The ecl was generated by using a cyclic square wave (10–20 Hz) with potential limits appropriate for the system under investigation. Ecl spectra were recorded on a Zenith microcomputer. The $Mo_6Cl_{14}^{2-}/W_6X_8Y_6^{2-}$ ecl spectra were resolved by employing a band shape analysis in which varying ratios of the steady-state emission spectra of the discrete cluster systems were added until their sum identically matched that of the observed ecl spectrum. Energy-partitioning values were obtained by normalizing the calculated ratio with the emission quantum yields of the two cluster systems. Errors in the partitioning ratio were determined from three independent measurements of the $Mo_6Cl_{14}^{2-}/W_6X_8Y_6^{2-}$ ecl spectrum.

Results and Discussion

Electrochemistry. Electrochemical properties of the molybdenum and tungsten halide cluster systems chosen for energy-paritioning studies are shown in Table I. Dichloromethane solutions of clusters at room temperature exhibit one-electron oxidation processes that are reversible; i_a/i_c ratios between 0.95 and 1.05 and linear plots of anodic and cathodic peak currents vs (scan rate)$^{1/2}$ are observed. Anodic to cathodic peak separations of the reversible cluster systems were comparable to that measured for ferrocene (125 mV), thereby establishing that deviations of ΔE_p from the theoretical value of 59 mV are due primarily to uncompensated cell resistance. Whereas the criteria for electrochemical reversibility are also fulfilled for the one-electron reduction of $Mo_6Cl_{14}^{2-}$ in CH_2Cl_2 at room temperature ($E_{1/2}$ = −1.70 V vs SCE), the one-electron reduction processes of each of the $W_6X_8Y_6^{2-}$ clusters are more negative than −2.2 V and therefore obscured by cathodic waves arising from solvent decomposition.

Electrogenerated Chemiluminescence. Ecl is observed from CH_2Cl_2 solutions containing the $Mo_6Cl_{14}^{2-}$ cluster resulting from simple annihilation of the electrochemically generated monoanion and trianion at the surface of a platinum electrode.[29] Conversely, the tungsten halide clusters listed in Table I produce weak or no ecl at a platinum electrode surface (the ecl efficiency, Φ_{ecl}, is $\leq 10^{-5}$) presumably due to the fact that the reduced cluster anion $W_6X_8Y_6^{3-}$ cannot cleanly be electrogenerated. However, the issue of interest here is not ecl produced from reactants electrogenerated from the same parent molecule but ecl originating from systems in which the electrochemical energy is partitioned between electronic excited states of distinct molecules. Because the $W_6X_8Y_6^{-/2-}$ redox couples are well negative of oxidation of $Mo_6Cl_{14}^{2-}$ and the $W_6X_8Y_6^{2-/3-}$ redox couples are more negative than the reduction of $Mo_6Cl_{14}^{2-}$, the following electron transfer reaction can be cleanly established by standard electrochemical techniques:[35]

$$Mo_6Cl_{14}^{3-} + W_6X_8Y_6^{-} \longrightarrow Mo_6Cl_{14}^{2-*} + W_6X_8Y_6^{2-} \quad (1a)$$

$$Mo_6Cl_{14}^{3-} + W_6X_8Y_6^{-} \longrightarrow Mo_6Cl_{14}^{2-} + W_6X_8Y_6^{2-*} \quad (1b)$$

$$Mo_6Cl_{14}^{3-} + W_6X_8Y_6^{-} \longrightarrow Mo_6Cl_{14}^{2-} + W_6X_8Y_6^{2-} \quad (2)$$

where ecl reactions 1a and 1b directly compete with ground-state production (reaction 2). Consistent with this analysis, chemiluminescence from CH_2Cl_2 solutions containing $Mo_6Cl_{14}^{2-}$ and $W_6X_8Y_6^{2-}$ ions is observed when the applied potential of a platinum electrode is stepped into the oxidation wave of $W_6X_8Y_6^{2-}$ and the reduction wave of $Mo_6Cl_{14}^{2-}$. Whereas the driving force to produce electronically excited $Mo_6Cl_{14}^{2-}$ ($Mo_6Cl_{14}^{2-*}$) or $W_6X_8Y_6^{2-}$ ($W_6X_8Y_6^{2-*}$) is energetically downhill for either reaction 1a or 1b, inspection of formal reduction potentials and the lowest excited-state energies of the $Mo_6Cl_{14}^{2-}$ and $W_6X_8Y_6^{2-}$ clusters listed in Tables I and II, respectively, shows that there is insufficient electrochemical excitation energy to produce both $Mo_6Cl_{14}^{2-*}$ and $W_6X_8Y_6^{2-*}$ cluster ions in a single electron transfer annihilation event.

Table II. Photophysical Properties of the Hexanuclear Cluster Ions Used in Ecl Partitioning Studies[a]

$M_6X_8Y_6^{2-}$ ion	$\lambda_{em,max}$/nm	τ/μs[b]	Φ_e[c]
$Mo_6Cl_{14}^{2-}$	766	160	0.18
$W_6Cl_8Br_6^{2-}$	814	4.4	0.030
$W_6Cl_{14}^{2-}$	833	2.2	0.015
$W_6Br_{14}^{2-}$	751	16	0.13
$W_6I_{14}^{2-}$	698	26	0.30
$W_6I_8Br_6^{2-}$	700	27	0.18

[a] All measurements performed on dichloromethane solution at 23 ± 1 °C. [b] Observed lifetime. [c] Emission quantum yield.

Inspection of the photophysical properties listed in Table II suggests that the formation of the excited states of these cluster ions can be spectroscopically distinguished owing to the distinct emission energies of the $Mo_6Cl_{14}^{2-}$ and $W_6X_8Y_6^{2-}$ ions. Accordingly, the partitioning ratio between reactions 1a and 1b can be determined directly from the ecl spectra of the $Mo_6Cl_{14}^{2-}/W_6X_8Y_6^{2-}$ systems if one assumes that subsequent energy transfer between the initially prepared excited-state products is unimportant. In order to assess the validity of this assumption, energy-transfer studies of the $Mo_6Cl_{14}^{2-}/W_6X_8Y_6^{2-}$ system were undertaken. The rate constants for luminescence quenching of $W_6X_8Y_6^{2-*}$ and $Mo_6Cl_{14}^{2-*}$ by $Mo_6Cl_{14}^{2-}$ and $W_6X_8Y_6^{2-}$, respectively

$$Mo_6Cl_{14}^{2-*} + W_6X_8Y_6^{2-} \longrightarrow Mo_6Cl_{14}^{2-} + W_6X_8Y_6^{2-*} \quad (3a)$$

$$Mo_6Cl_{14}^{2-} + W_6X_8Y_6^{2-*} \longrightarrow Mo_6Cl_{14}^{2-*} + W_6X_8Y_6^{2-} \quad (3b)$$

were deduced from classical Stern–Volmer analysis of the $Mo_6Cl_{14}^{2-}$ and $W_6X_8Y_6^{2-}$ lifetimes. The results of these quenching studies are summarized in Table III. Because both cluster ions emit, individual lifetimes were determined from a multiexponential

(35) Faulkner, L. R.; Bard, A. J. *J. Electroanal. Chem. Interfacial Electrochem.* **1977**, *10*, 1–95.

Table III. Rate Constants for Energy-Transfer Quenching of $M_6X_8Y_6^{2-}$ Hexanuclear Clusters[a]

lumophore	quencher	$\Delta G/V$[b]	$k_q/M^{-1}\ s^{-1}$[c]
$W_6I_8Br_6^{2-}$	$Mo_6Cl_{14}^{2-}$	−0.28	9×10^7
$W_6I_{14}^{2-}$	$Mo_6Cl_{14}^{2-}$	−0.26	2×10^7
$Mo_6Cl_{14}^{2-}$	$W_6Cl_{14}^{2-}$	−0.15	5×10^4
$Mo_6Cl_{14}^{2-}$	$W_6Cl_8Br_6^{2-}$	−0.10	$<10^4$
$W_6Br_{14}^{2-}$	$Mo_6Cl_{14}^{2-}$	−0.02	$<10^4$

[a] All measurements were made in dichloromethane containing 0.1 M tetrabutylammonium hexafluorophosphate at 23 ± 1 °C. For a given cluster pair, the exergonic energy-transfer reaction is listed. [b] The driving force for energy transfer was determined from estimation of the 0–0 energy of the low-temperature (10 K) luminescence spectra of crystalline solids: $\Delta G = -[E_{0,0}(\text{lumophore}) - E_{0,0}(\text{quencher})]$. [c] Quenching rate constants determined from Stern–Volmer analysis of the cluster lifetimes.

fit of the luminescence decay with the equation $y = ae^{-t/\tau_1} + be^{-t/\tau_2}$ by using the general nonlinear curve-fitting program Kinfit[36] where a and b represent the fractions of total emission decay described by the excited-state lifetimes, τ_1 and τ_2, respectively. Convergence of fit, monitored by the sum of the squares of the residuals, yields values for a, b, τ_1, and τ_2. Obviously, for an individual reaction pair only one energy-transfer reaction, (3a) or (3b), will be energetically favored. Classical energy-transfer treatments[37,38] predict the exothermic reaction will predominate and that its endergonic counterpart will be comparably inefficient. On this basis, we expect that if energy transfer is important, then only one cluster lifetime will be attenuated. Quenching results are consistent with this analysis. For example, consider the $Mo_6Cl_{14}^{2-}/W_6I_{14}^{2-}$ system. For this cluster pair, reaction 3a is endergonic and Stern–Volmer quenching experiments show that the $Mo_6Cl_{14}^{2-}$ lifetime is invariant with the $W_6I_{14}^{2-}$ concentration. Conversely, a favorable driving force of −0.15 V for reaction 3b is manifested in quenching of the $W_6I_{14}^{2-}$ lifetime with a rate of $10^7\ M^{-1}\ s^{-1}$. Thus for the $Mo_6Cl_{14}^{2-}/W_6I_{14}^{2-}$ system, $Mo_6Cl_{14}^{2-}$ is the quencher and its excited-state lifetime is constant whereas $W_6I_{14}^{2-}$ is the lumophore and its excited-state lifetime follows a classical Stern–Volmer dependence. As presented in Table III, that the largest quenching rates for the $Mo_6Cl_{14}^{2-}/W_6X_8Y_6^{2-}$ mixed-cluster systems are 2 orders of magnitude smaller than the diffusion-controlled rate, despite significant driving forces of some of the reactions, is consistent with the results of previous studies of the energy-transfer reactions of these cluster ions.[39] The good acceptor/donor orbital overlap required for efficient energy transfer is not fulfilled for the cluster ions because the metal-localized emissive excited state is sterically shielded by the halide coordination sphere. Thus energy transfer between mixed-cluster pairs is inefficient and the measured excited-state production yields of the $Mo_6Cl_{14}^{3-}/W_6X_8Y_6^{-}$ annihilation reactions should therefore accurately reflect the partitioning of the electrochemical excitation energy between cluster excited states.

Partitioning between reaction pathways 1a and 1b for the $Mo_6Cl_{14}^{2-}/W_6Cl_8Br_6^{2-}$, $-W_6I_8Br_6^{2-}$, and $-W_6I_{14}^{2-}$ mixed-cluster systems can be determined directly from inspection of ecl spectra. The exemplary ecl spectrum of the $Mo_6Cl_{14}^{2-}/W_6I_{14}^{2-}$ system is shown in Figure 1a. Comparison of the ecl spectrum of the mixed-cluster system to that for the steady-state emission spectra of the individual ions clearly, also reproduced in Figure 1a, reveals an ecl profile composed of $Mo_6Cl_{14}^{2-}$ and $W_6I_{14}^{2-}$ emissions. The relative contribution of $Mo_6Cl_{14}^{2-}$ and $W_6I_{14}^{2-}$ emission (χ_{Mo_6} and χ_{W_6}, respectively) can be ascertained by fitting the ecl spectrum with the emission spectra of the individual ions as shown in Figure 1b. By normalizing this quantity with the emission quantum yields of the cluster ions (Φ_{Mo_6} and Φ_{W_6}), one can obtain the ratio for

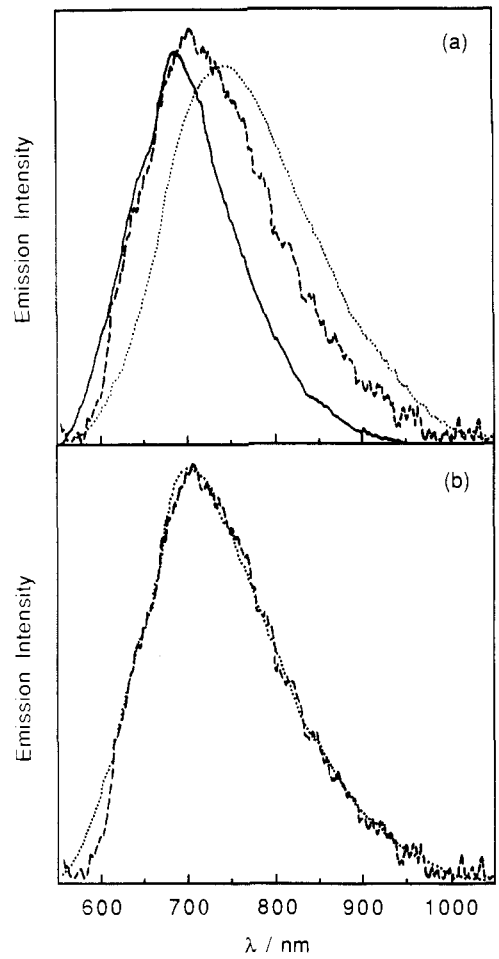

Figure 1. (a) Electrogenerated chemiluminescence spectrum of $Mo_6Cl_{14}^{2-}/W_6I_{14}^{2-}$ (---) and steady-state emission spectra of $Mo_6Cl_{14}^{2-}$ (···) and $W_6I_{14}^{2-}$ (—) in CH_2Cl_2 (μ = 0.1 M (NBu_4PF_6) at 23 ± 1 °C). (b) $Mo_6Cl_{14}^{2-}/W_6I_{14}^{2-}$ ecl spectrum (---) fit to the sum of the appropriate ratio of the $Mo_6Cl_{14}^{2-}$ and $W_6I_{14}^{2-}$ emission spectra (···). The ecl and steady-state emission spectra are not corrected for the instrument response of the spectrometer.

partitioning the electrochemical excitation energy between reactions 1a and 1b

$$P_R\left(\frac{1a}{1b}\right) = \left(\frac{\chi_{Mo_6}}{\chi_{W_6}}\right)\left(\frac{\Phi_{W_6}}{\Phi_{Mo_6}}\right) \qquad (4)$$

Evaluation of eq 4 with a χ_{Mo_6}/χ_{W_6} ratio of 0.90, as measured from Figure 1b, and the previously determined $Mo_6Cl_{14}^{2-}$ and $W_6I_{14}^{2-}$ emission quantum yields gives P_R = 0.60:0.40. Similar analyses of the ecl spectra of the $Mo_6Cl_{14}^{2-}/W_6Cl_8Br_6^{2-}$ and $-W_6I_8Br_6^{2-}$ systems (χ_{Mo_6}/χ_{W_6} = 6.0 and 2.3, respectively) yield partitioning ratios of 0.50:0.50 and 0.70:0.30, respectively.

For the case of the $Mo_6Cl_{14}^{2-}/W_6Cl_{14}^{2-}$ and $-W_6Br_{14}^{2-}$ systems, partitioning ratios cannot reliably be evaluated on the basis of ecl spectra, but can be only indirectly determined from analysis of the overall ecl efficiency of the mixed-cluster system, which is given by

$$\Phi_{ecl} = \eta_{es}(1a)\ \Phi_{Mo_6} + \eta_{es}(1b)\ \Phi_{W_6} \qquad (5)$$

where $\eta_{es}(1a)$ and $\eta_{es}(1b)$ are the excited-state production yields of $Mo_6Cl_{14}^{2-*}$ and $W_6X_8Y_6^{2-*}$, and Φ_{Mo_6} and Φ_{W_6} have been previously defined. For the case of the $Mo_6Cl_{14}^{2-}/W_6Cl_{14}^{2-}$ system, owing to the small emission quantum yield of $W_6Cl_{14}^{2-}$ as compared to $Mo_6Cl_{14}^{2-}$, ecl from the former ion will be effectively masked by that of the latter; practically, eq 5 reduces to $\Phi_{ecl} = \eta_{es}(1a)\ \Phi_{Mo_6}$ and ecl from the $W_6Cl_{14}^{2-}$ ion will be detected by our instrument only if $\eta_{es}(1b) \geq 5\eta_{es}(1a)$ (i.e. $\chi_{Mo_6}/\chi_{W_6} \leq 0.17$). To this end, it is not surprising that the ecl spectrum resulting from annihilation of $Mo_6Cl_{14}^{3-}$ and $W_6Cl_{14}^{-}$ identically matches

(36) Dye, J. L.; Nicely, V. A. *J. Chem. Educ.* **1971**, *48*, 443–448.
(37) Balzani, V.; Bolletta, F.; Scandola, F. *J. Am. Chem. Soc.* **1980**, *102*, 2152–2163.
(38) Endicott, J. F. *Acc. Chem. Res.* **1988**, *21*, 59–66.
(39) Jackson, J. A.; Turro, C.; Newsham, M. D.; Nocera, D. G. *J. Phys. Chem.* **1990**, *94*, 4500–4507.

the steady-state emission spectrum of $Mo_6Cl_{14}^{2-}$. One explanation for this observation is that $W_6Cl_{14}^{-}$ simply acts as an electron acceptor and only the $Mo_6Cl_{14}^{3-}$ ion is electrochemically excited. However, our previous studies[25a] on the ecl chemistry of the $Mo_6Cl_{14}^{3-}$ and organic acceptors (A^+) suggest otherwise. Annihilation of the $Mo_6Cl_{14}^{3-}$ ion by aromatic radical cations possessing reduction potentials similar to that of the $W_6Cl_{14}^{-}$ ion yields ecl efficiencies twice that of this mixed-cluster system ($\Phi_{ecl}(Mo_6Cl_{14}^{3-}/A^+) = 0.10$; $\Phi_{ecl}(Mo_6Cl_{14}^{3-}/W_6Cl_{14}^{-}) = 0.05$). Alternatively, our observation of $\Phi_{ecl}(Mo_6Cl_{14}^{3-}/W_6Cl_{14}^{-}) = {}^1/_2\Phi_{ecl}(Mo_6Cl_{14}^{3-}/A^+)$ is consistent with an annihilation reaction in which half of the electrochemical excitation energy is distributed to the $W_6Cl_{14}^{2-}$ cluster excited state. This conclusion is consistent with the results of $Mo_6Cl_{14}^{2-}/W_6Cl_8Br_6^{2-}$ ecl, which as described above, exhibit a partitioning ratio of unity. Owing to the electronic and structural similarities of the $W_6Cl_{14}^{2-}$ and $W_6Cl_8Br_6^{2-}$ ions, our observation of similar partitioning ratios for their ecl reaction of their oxidized ions with $Mo_6Cl_{14}^{2-}$ seems reasonable. For the case of the $Mo_6Cl_{14}^{2-}/W_6Br_{14}^{2-}$ mixed-cluster system, the emission bands of the cluster ions are too close in energy [$\Delta(E_{em,max}(Mo_6Cl_{14}^{2-}) - E_{em,max}(W_6Br_{14}^{2-})) = 15$ nm] to permit the individual ecl spectra to be discerned. Comparison of the $Mo_6Cl_{14}^{2-}/W_6Br_{14}^{2-}$ electron transfer to that of $Mo_6Cl_{14}^{3-}/A^+$ is again enlightening. A measured ecl efficiency of 0.075 for the mixed-cluster system represents a 25% decrease over that for the energetically equivalent $Mo_6Cl_{14}^{3-}/A^+$ system ($\Phi_{ecl} = 0.10$). This decrease can precisely be attributed to the decreased quantum yield of the $W_6Br_{14}^{2-}$ ion with respect to $Mo_6Cl_{14}^{2-}$.

Although our determination of the partitioning ratios for the $Mo_6Cl_{14}^{2-}/W_6Cl_8Br_6^{2-}$ and $-W_6Br_{14}^{2-}$ systems is not unequivocal owing to our tacit assumption that the $Mo_6Cl_{14}^{3-}/A^+$ annihilation can be used as a reference for mixed-cluster ecl, it is significant that the result of equal partitioning of the electrochemical excitation energy is similar to that directly measured for the partitioning ratios of the $Mo_6Cl_{14}^{2-}/W_6Cl_8Br_6^{2-}$, $-W_6I_8Br_6^{2-}$, and $-W_6I_{14}^{2-}$ mixed-cluster systems. To this end, a particularly satisfying aspect of the results of the partitioning experiments is that the free energy dependence of $Mo_6Cl_{14}^{2-}$ excited-state production is independent of the nature of the electron acceptor. The free energy dependence of the excited-state production of $Mo_6Cl_{14}^{2-}$ from the reaction of $Mo_6Cl_{14}^{3-}$ with aromatic amines and $W_6X_8Y_6^{2-}$ acceptors is shown in Figure 2. In the former system, the population of the lowest energy acceptor excited state is an energetically unfavorable process and thus the electrochemical excitation energy is channeled exclusively via the $Mo_6Cl_{14}^{2-}$ excited state whereas in the latter system the excitation energy is shared equally between the $Mo_6Cl_{14}^{2-}$ and acceptor excited states. This partitioning of excited-state energy is reflected in the fact that the $Mo_6Cl_{14}^{2-*}$ production yield for the mixed-cluster system at a given free energy is half that for $Mo_6Cl_{14}^{3-}/A^+$ annihilation. Acknowledging this expected difference in absolute production yields, it is noteworthy that, for a given series of structurally and electronically similar acceptors, the free energy dependence for the production of $Mo_6Cl_{14}^{2-*}$ exhibits parallel trends across the organic and $W_6X_8Y_6^{2-}$ acceptor series. This result demonstrates that the mechanism for excited-state production is independent of whether the electrochemical excitation energy is distributed between one or two excited states.

Electron Transfer. The electron-transfer properties of the oxidized and reduced clusters bear directly on the equal partitioning of electrochemical excitation energy between $Mo_6Cl_{14}^{2-}$ and $W_6X_8Y_6^{2-}$. An electron-transfer model for the annihilation of $Mo_6Cl_{14}^{3-}$ by $W_6X_8Y_6^{-}$ is described as follows:

$$Mo_6Cl_{14}^{3-} + W_6X_8Y_6^{-} \underset{k_{-d}}{\overset{k_d}{\rightleftharpoons}} Mo_6Cl_{14}^{3-}\cdots W_6X_8Y_6^{-} \quad (6)$$

$$Mo_6Cl_{14}^{3-}\cdots W_6X_8Y_6^{-} \xrightarrow{k_{Mo_6^*}} Mo_6Cl_{14}^{2-*} + W_6X_8Y_6^{2-} \quad (7a)$$

$$Mo_6Cl_{14}^{3-}\cdots W_6X_8Y_6^{-} \xrightarrow{k_{W_6^*}} Mo_6Cl_{14}^{2-} + W_6X_8Y_6^{2-*} \quad (7b)$$

$$Mo_6Cl_{14}^{3-}\cdots W_6X_8Y_6^{-} \xrightarrow{k_{gs}} Mo_6Cl_{14}^{2-} + W_6X_8Y_6^{2-} \quad (8)$$

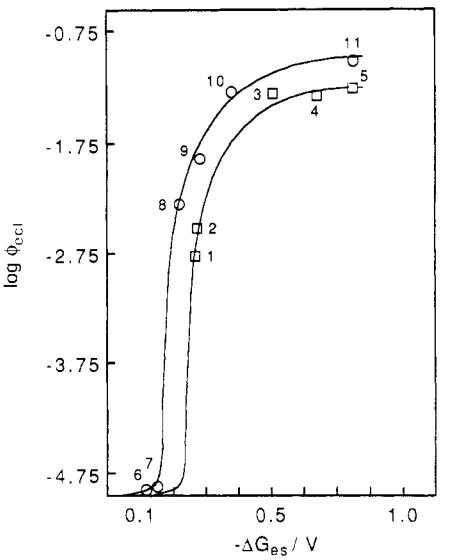

Figure 2. Plot of the logarithm of the excited-state production yield of $Mo_6Cl_{14}^{2-}$ in the annihilation reactions of $Mo_6Cl_{14}^{3-}$ with the cluster acceptors $W_6X_8Y_6^{-}$ (□) and aromatic amine acceptors (○) vs the free energy driving force for excited-state production. The data for the $Mo_6Cl_{14}^{3-}$/aromatic amine acceptor systems are taken from ref 25a. The numbering scheme is as follows: $W_6I_{14}^{2-}$ (1); $W_6I_8Br_6^{2-}$ (2); $W_6Br_{14}^{2-}$ (3); $W_6Cl_{14}^{2-}$ (4); $W_6Cl_8Br_6^{2-}$ (5); phenothiazine (6); bis(methoxyphenyl)amine (7); 10-methylphenothiazine (8); *N*,*N*-dimethyl-*p*-toluidine (9); tri-*p*-tolylamine (10); tris(4-bromophenyl)amine (11).

where k_d and k_{-d} are diffusional rate constants, $k_{Mo_6^*}$ and $k_{W_6^*}$ are the rate constants for $Mo_6Cl_{14}^{2-}$ and $W_6X_8Y_6^{2-}$ excited-state production, and k_{gs} describes the rate for direct production of ground-state molecules. Because $Mo_6Cl_{14}^{2-*}$ and $W_6X_8Y_6^{2-*}$ are competitively produced from the same reactants, the partitioning ratio should be independent of k_d, k_{-d}, and k_{gs}, and therefore insight into the factors governing electrochemical partitioning in the mixed-cluster systems will follow directly from analysis of $k_{Mo_6^*}$ and $k_{W_6^*}$.

The excited-state reaction rates $k_{Mo_6^*}$ and $k_{W_6^*}$ are given by the Marcus expression[40]

$$k_{Mo_6^*,W_6^*} = \left(\frac{2H_{AB}^2}{h}\right)\left(\frac{\pi^3}{\lambda k_B T}\right)^{1/2} \exp\left[\frac{-(\lambda + \Delta G_{et})^2}{4\lambda k_B T}\right] \quad (9)$$

where H_{AB} is the electronic coupling matrix element, λ is the sum of the inner (λ_i) and outer sphere (λ_o) reorganizational energies, and ΔG_{et} is the free energy driving force of reactions 7a and 7b. The nearly equal production of $Mo_6Cl_{14}^{2-*}$ and $W_6X_8Y_6^{2-*}$ in the mixed-cluster ecl reaction implies that $k_{Mo_6^*} \approx k_{W_6^*}$. Our previous studies of $M_6X_{14}^{2-}$ ecl establish that excited-state production from either the oxidized or the reduced ion is independent of ΔG_{et} at driving forces just negative of the ecl threshold energy ($\Delta G_{et} < -0.05$).[25a] Moreover, λ_o is independent of which reactant, $Mo_6Cl_{14}^{2-}$ and $W_6X_8Y_6^{2-}$, is converted to the excited state for a given mixture-cluster system. Therefore, partitioning between reaction pathways 7a and 7b depends exclusively on H_{AB} and the inner-sphere reorganizational energy.

The roles of H_{AB} and λ_i in determining the partitioning can be understood within the context of a description of the hexanuclear cluster's frontier molecular orbitals. Spectroscopic[41] and theoretical studies[42,43] predict the HOMO and LUMO to be primarily metal in character and to possess molecular symmetries e_g and a_{2g}, respectively. On this basis, the annihilation reaction between $Mo_6Cl_{14}^{3-}$ and $W_6X_8Y_6^{-}$ is described by the molecular orbital

(40) Marcus, R. A.; Sutin, N. *Biochim. Biophys. Acta* **1985**, *811*, 265–322.
(41) Maverick, A. W.; Najdzionek, J. S.; MacKenzie, D.; Nocera, D. G.; Gray, H. B. *J. Am. Chem. Soc.* **1983**, *105*, 1878–1882.
(42) Hughbanks, T.; Hoffman, R. *J. Am. Chem. Soc.* **1983**, *105*, 1150–1162.
(43) Seifert, G.; Grossman, G.; Muller, H. *J. Mol. Struct.* **1980**, *64*, 93–102.

Table IV. Reduction Potentials and Rate Constants for the Reductive Quenching of $Mo_6Cl_{14}^{2-*}$ by Aromatic Amine Donors[a]

	lumophore	donor (D)	$E_{1/2}/V^b$	$\Delta G_{et}/V^c$	$k_q/M^{-1}\ s^{-1}$ [d]
1	$Mo_6Cl_{14}^{2-}$	bis(methoxyphenyl)amine	+0.51	+0.07	2.8×10^8
2	$Mo_6Cl_{14}^{2-}$	phenothiazine	+0.52	+0.08	1.9×10^8
3	$Mo_6Cl_{14}^{2-}$	10-methylphenothiazine	+0.63	+0.19	2.4×10^7
4	$Mo_6Cl_{14}^{2-}$	*N,N*-dimethyl-*p*-toluidine	+0.65	+0.21	2.0×10^7
5	$Mo_6Cl_{14}^{2-}$	tri-*p*-tolylamine	+0.69	+0.25	8.0×10^6

[a] All measurements were made in dichloromethane containing 0.1 M tetrabutylammonium hexafluorophosphate at 23 ± 1 °C. [b] As reduction potentials for the $D^{+/0}$ couple vs SCE. [c] Standard free energy change for the electron-transfer reaction of $Mo_6Cl_{14}^{2-*}$ with D: $\Delta G_{et} = -[E_{1/2}(Mo_6Cl_{14}^{2-*/3-}) - E_{1/2}(D^{+/3})]$; $E_{1/2}(Mo_6Cl_{14}^{2-*/3-}) = 0.44$ V vs SCE. [d] Quenching rate constants determined from lifetime measurements.

Table V. Reduction Potentials and Rate Constants for the Oxidative Quenching of $M_6X_{14}^{2-*}$ by Aromatic Nitro and Quinone Donors[a]

	lumophore	acceptor (A)	$E_{1/2}/V^b$	$\Delta G_{et}/V^c$	$k_q/M^{-1}\ s^{-1}$ [d]
1	$Mo_6Br_{14}^{2-}$	3,5-dichloro-*p*-benzoquinone	−0.34	−0.25	9.6×10^9
2	$W_6Br_{14}^{2-}$	*p*-dinitrobenzene	−0.75	−0.14	3.0×10^9
3	$Mo_6Cl_{14}^{2-}$	3,5-dichloro-*p*-benzoquinone	−0.34	−0.04	9.0×10^8
4	$W_6Cl_{14}^{2-}$	*p*-dinitrobenzene	−0.75	+0.11	3.0×10^7
5	$Mo_6Cl_{14}^{2-}$	*p*-benzoquinone	−0.55	+0.17	2.3×10^6

[a] All measurements were made in acetonitrile containing 0.1 M tetrabutylammonium hexafluorophosphate at 23 ± 1 °C. [b] As reduction potentials for the $A^{0/-}$ couple vs SCE. [c] Standard free energy change for the electron-transfer reaction of $M_6X_{14}^{2-*}$ with A: $\Delta G_{et} = -[E_{1/2}(A^{0/-}) - E_{1/2}(M_6X_{14}^{-/2-*})]$; $E_{1/2}(Mo_6Cl_{14}^{-/2-*}) = -0.38$ V vs SCE, $E_{1/2}(Mo_6Br_{14}^{-/2-*}) = -0.59$ V vs SCE, $E_{1/2}(W_6Cl_{14}^{-/2-*}) = -0.64$ V vs SCE, and $E_{1/2}(W_6Br_{14}^{-/2-*}) = -0.89$ V vs SCE. [d] Quenching rate constants determined from lifetime measurements.

representation depicted in Figure 3. An important result to emerge from this description is that the two excited-state pathways are electronically distinct. Production of $Mo_6Cl_{14}^{2-*}$ from $Mo_6Cl_{14}^{3-}$ involves the transfer of an electron from an e_g orbital of $Mo_6Cl_{14}^{3-}$ to the e_g orbital of the $W_6X_8Y_6^-$ ion. Conversely, transfer of an electron from the a_{2g} orbital of $Mo_6Cl_{14}^{3-}$ to the a_{2g} orbital on the $W_6X_8Y_6^-$ ion produces electronically excited $W_6X_8Y_6^{2-*}$. We can only account for our observation of comparable excited-state rates, $k_{Mo_6^*} \approx k_{W_6^*}$, if (i) reactions 7a and 7b possess similar values of both H_{AB} and λ_i or (ii) the contributions of these parameters in eq 9 effectively counterbalance each other such that equal rates are obtained.

Differences in H_{AB} for the production of $M_6X_8Y_6^{2-*}$ from either $M_6X_8Y_6^-$ or $M_6X_8Y_6^{3-}$ will arise if the respective orbital overlap of the a_{2g} orbitals is different from that of the e_g orbitals. This case is unlikely for the mixed-cluster ecl system. The e_g HOMO and a_{2g} LUMO molecular orbitals are constructed from linear combinations of d_{xy} orbitals of adjacent metal atoms.[44] The molecular orbitals are confined to a cube that inscribes the octahedral metal atoms of the cluster unit. Owing to the similar radial distributions of these metal-based orbitals, exchange of an electron between a_{2g} (reaction 7b) or e_g (reaction 7a) orbitals of the cluster core should be characterized by similar values of H_{AB}.[25a] On this basis, our observation of equal partitioning implies similar λ_i's for the conversion of $Mo_6X_8Y_6^{3-}$ or $W_6X_8Y_6^-$ to their respective excited states.

The λ_i energies associated with electron-exchange reactions involving the a_{2g} and e_g orbitals can independently be measured by electron-transfer-quenching studies of $M_6X_8Y_6^{2-*}$ with a series of organic electron donors and acceptors. In the $M_6X_8Y_6^{2-*}$ electronic excited state, a reducing electron resides in the a_{2g} orbital and an oxidizing hole is present in the degenerate e_g orbital set. Accordingly, oxidative quenching of the excited state involves the donation of an electron from its a_{2g} orbital to an acceptor molecule A to produce the reduced radical A^- and the oxidized cluster $M_6X_8Y_6^-$. Alternatively, in the presence of donor molecules D, an electron is transferred to the cluster's e_g orbital to produce oxidized D^+ and reduced cluster $M_6X_8Y_6^{3-}$. The λ_i value measured for the conversion of $M_6X_8Y_6^{2-*}$ to $M_6X_8Y_6^{3-}$ in reductive quenching studies is related directly to the generation of $M_6X_8Y_6^{2-*}$ from a $M_6X_8Y_6^{3-}$ parentage in the ecl annihilation reaction. Conversely, the cluster's contribution to the measured inner-sphere reorganizational energy of electron transfer quenching of $M_6X_8Y_6^{2-*}$ luminescence by A is directly related to λ_i for the ecl conversion of $M_6X_8Y_6^-$ to $M_6X_8Y_6^{2-*}$. In order to parallel

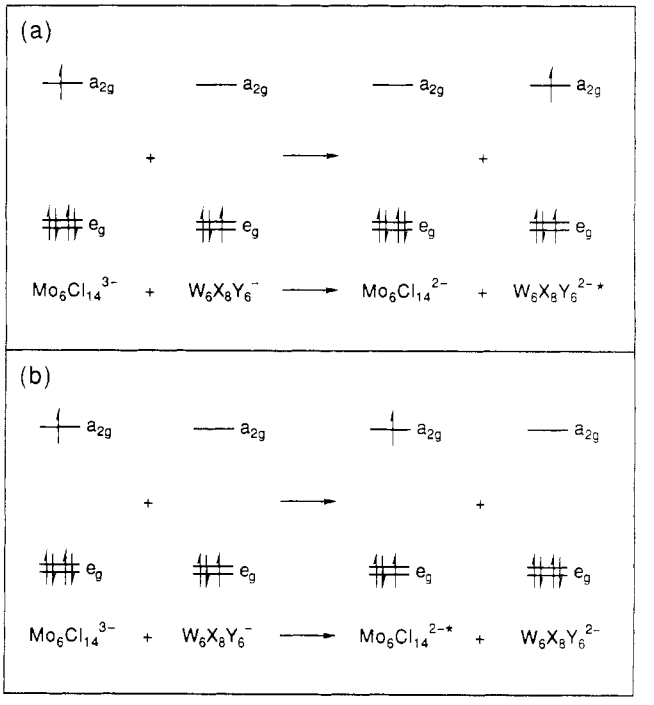

Figure 3. Molecular orbital description for the electron-transfer annihilation of $Mo_6Cl_{14}^{3-}$ with $W_6X_8Y_6^-$ to give electronically excited (a) $W_6X_8Y_6^{2-}$ or (b) $Mo_6Cl_{14}^{2-}$.

the ecl reactions described by reactions 7a and 7b as closely as possible, the reductive quenching of $Mo_6Cl_{14}^{2-*}$ by aromatic amine donors (D) (reaction 10) and the oxidative quenching of $M_6X_8Y_6^{2-*}$ by nitroaromatics and quinones (reaction 11) were

$$Mo_6Cl_{14}^{2-*} + D \longrightarrow Mo_6Cl_{14}^{3-} + D^+ \quad (10)$$

$$M_6X_8Y_6^{2-*} + A \longrightarrow M_6X_8Y_6^- + A^- \quad (11)$$

investigated. In the case of the oxidative quenching reaction, large $W_6X_8Y_6^{-/2-*}$ excited-state potentials are manifested in nearly diffusion-controlled quenching rates. Thus the measurement of sufficient rate constant data below approaching the diffusion-controlled limit required us to include oxidative quenching reactions of the $Mo_6X_8Y_6^{2-*}$ in addition to the $W_6X_8Y_6^{2-*}$ cluster excited states. The quenching rate constants, as determined from Stern–Volmer analysis of the lifetime, for reactions 10 and 11

(44) Zietlow, T. C.; Hopkins, M. D.; Gray, H. B. *J. Solid State Chem.* **1985**, *57*, 112–119.

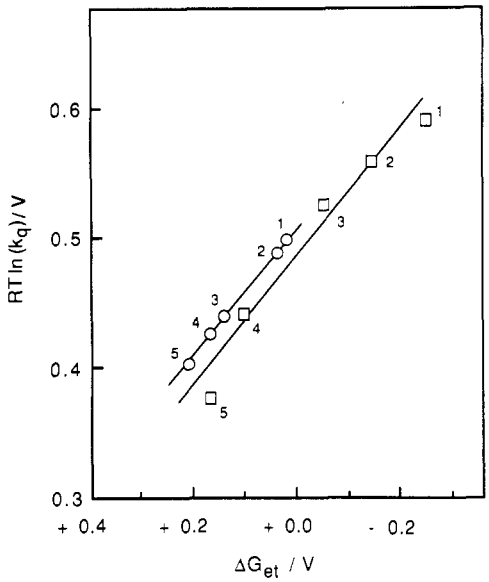

Figure 4. Plot of $RT \ln k_q$ vs the free energy driving force for electron-transfer ΔG_{et} for the quenching of $Mo_6Cl_{14}^{2-*}$ by aromatic donors (○) and acceptors (□) in CH_3CN at 23 ± 1 °C. The quencher numbering scheme is given in Tables IV and V, respectively.

are summarized in Tables IV and V, respectively. From these data, λ_i can be evaluated with eq 12,

$$RT \ln k_{Mo_6^{*},W_6^{*}} = \left\{ RT \ln \left[\frac{2H_{AB}^2}{h} \left(\frac{\pi^3}{\lambda k_B T} \right)^{1/2} \right] - \frac{\lambda}{4} \right\} - \frac{1}{2}\Delta G_{et} \quad (12)$$

which is obtained by rearranging the electron-transfer rate expression of eq 9. The quadratic free energy term of eq 9 has not been included owing to its relatively small contribution to the overall observed quenching rate at low driving forces. Consequently, eq 12 predicts a linear plot of $RT \ln k_q$ vs ΔG_{et} with a slope of −0.5 and an intercept equal to the bracketed term.[45-47]

Plots of the dependence of the logarithmic rates on the free energy driving force of acceptor and donor quenching pathways are shown in Figure 4. The linear dependence of the rate constant on ΔG_{et} and slopes of −0.49 and −0.51 for $M_6X_8Y_6^{2-*}$/A and $Mo_6Cl_{14}^{2-*}$/D systems, respectively, agree well with theory. By assuming adiabatic electron transfer (H_{AB} = 150 cm^{-1}), overall reorganizational energies λ ($=\lambda_o + \lambda_i$) of 1.11 and 1.01 eV are calculated from the intercepts of Figure 4, respectively.[48] The outer-sphere contribution to the overall reorganizational energy is given by eq 13[49] where a_i and a_j are the radii of the cluster and

$$\lambda_o = (\Delta e^2)\left(\frac{1}{2a_i} + \frac{1}{2a_j} - \frac{1}{r_{ij}2} \right)\left(\frac{1}{\epsilon_s} - \frac{1}{\epsilon_{op}} \right) \quad (13)$$

acceptor/donor reactants, r is the distance over which electron transfer occurs, and ϵ_s and ϵ_{op} are the static and optical dielectric constants of the solvent. The structural similarities between the acceptors and donors and between the $Mo_6Cl_{14}^{2-}$ and $W_6X_8Y_6^{2-}$ cluster ions is manifested in a nearly constant value of λ_o = 0.85 ± 0.05 eV for reactions 10a and 10b.[50] Hence λ_i values of 0.25 and 0.15 eV are obtained for quenching reactions 7a and 7b, respectively. These values, predicated on adiabatic electron transfer, represent upper limits of λ_i. From eq 12, λ and consequently λ_i will decrease with increasing nonadiabaticity of the electron-transfer reaction. Thus the observation of small and equal λ_i's ($0 < \lambda_i < 0.25$ eV) for reactions 7a and 7b is preserved even if the electron transfer reflects nonadiabatic contributions. EPR line broadening experiments have shown[51] that the overall reorganizational energies for the self-exchange electron-transfer reactions of aromatic amines and nitroaromatics is <0.05 eV and, hence, the experimentally determined values of λ_i for quenching reactions 7a and 7b directly reflect the inner-sphere reorganizational energies associated with $M_6X_8Y_6^{2-*}/M_6X_8Y_6^{-}$ and $M_6X_8Y_6^{2-*}/M_6X_8Y_6^{3-}$ conversions, respectively. Changes in metal–metal bond lengths and angles resulting from the population and depopulation of the a_{2g} and e_g orbitals will be distributed over the entire metal octahedral core. Consequently, small inner-sphere reorganizational energies are associated with the excited-state one-electron processes of $M_6X_8Y_6^{2-}$ ions.

Thus our observation that the electrochemical excitation energy of the $Mo_6Cl_{14}^{3-}/W_6X_8Y_6^{-}$ annihilation reaction is channeled to either reactant with equal probability is directly attributable to electronic similarities of the HOMO and LUMO orbitals of the $M_6X_8Y_6^{2-}$ ions, which are manifested in similar electronic coupling and inner-sphere reorganizational energies for the two excited-state pathways. This observation is consistent with earlier results which show that the excited state of $Mo_6Cl_{14}^{2-*}$ is produced with nearly equal efficiency from $Mo_6Cl_{14}^{-}$ or $Mo_6Cl_{14}^{3-}$ in the presence of donors or acceptors, respectively. Moreover, inasmuch as the electron-transfer chemistry of the $[M_6X_8]Y_6^{-}$ and $[M_6X_8]Y_6^{3-}$ ions is reflected by $W_6X_8Y_6^{-}$ and $Mo_6Cl_{14}^{3-}$, the results of the mixed-cluster systems establish that the monoanion and trianion contribute equally to the production of electronically excited clusters in the annihilation of reactants electrogenerated from the same parent cluster.

Acknowledgment. Financial support from the National Science Foundation (Grant CHE-8705871) is acknowledged. Mass spectral data were obtained at the Michigan State University Mass Spectrometry Facility, which is supported, in part, by a grant (DRR-00480) from the Biotechnology Resources Branch, Division of Research Resources, National Institutes of Health. D.G.N. gratefully acknowledges a Presidential Young Investigator Award administered by the National Science Foundation, and financial assistance from the Dow Chemical Co. is also gratefully acknowledged.

Registry No. WCl_6, 13283-01-7; Al, 7429-90-5; $(NBu_4)_2W_6Cl_{14}$, 84648-02-2; $W_6Br_{12}(HOCH_2CH_3)_2$, 12144-66-0; $(NBu_4)_2W_6Br_{14}$, 96390-92-0; $K_2W_6Cl_{14}$, 128659-10-9; W_6I_{12}, 12298-70-3; $(NBu_4)_2W_6I_{14}$, 27680-20-2; $Mo_6Cl_{14}^{2-}$, 51364-21-7; $W_6Cl_8Br_6^{2-}$, 47021-00-1; $W_6Cl_{14}^{2-}$, 47021-01-2; $W_6Br_{14}^{2-}$, 88477-00-3; $W_6I_{14}^{2-}$, 47021-02-3; $W_6I_8Br_6^{2-}$, 126926-89-4; tungsten dichloride, 13470-12-7.

(45) Scandola, F.; Balzani, V.; Schuster, G. B. *J. Am. Chem. Soc.* **1981**, *103*, 2519–2523.
(46) (a) Nocera, D. G.; Gray, H. B. *J. Am. Chem. Soc.* **1981**, *103*, 7349–7350. (b) Marshall, J. L.; Stobart, S. R.; Gray, H. B. *J. Am. Chem. Soc.* **1984**, *106*, 3027–3029.
(47) Kavarnos, G. J.; Turro, N. J. *Chem. Rev.* **1986**, *86*, 401–449 and references therein.
(48) Equation 12 was evaluated for H_{AB} = 0.02 eV, and ΔG_{et} was corrected for product work term contributions (w_p = −0.11 eV and +0.04 eV for quenching reactions 10 and 11, respectively).
(49) (a) Marcus, R. A. *Annu. Rev. Phys. Chem.* **1964**, *15*, 155–196. (b) Marcus, R. A. *J. Chem. Phys.* **1956**, *24*, 966–978.
(50) The electron-transfer distance r_{ij} was determined by calculating the radii equivalent to the sphere of equal volume, $a_j = {}^1/_2(d_1d_2d_3)^{1/3}$ for all acceptors and donors used in ecl studies. d_i represents the van der Waals diameter along the molecular axes.
(51) Kowert, B. A.; Marcoux, L.; Bard, A. J. *J. Am. Chem. Soc.* **1972**, *94*, 5538–5550.